JACS
JOURNAL OF THE AMERICAN CHEMICAL SOCIETY
pubs.acs.org/JACS
Article

Taming Molecular Folding: Anion-Templated Foldamers with Tunable Quaternary Structures

Eric A. John, Asia Marie S. Riel, Lianne H. E. Wieske, Debmalya Ray, Daniel A. Decato, Madeleine Boller, Zoltan Takacs, Máté Erdélyi, Vyacheslav S. Bryantsev,* and Orion B. Berryman*

Cite This: J. Am. Chem. Soc. 2024, 146, 16419−16427

ABSTRACT: Higher-order foldamers represent a unique class of supramolecules at the forefront of molecular design. Herein we control quaternary folding using a novel approach that combines halogen bonding (XBing) and hydrogen bonding (HBing). We present the first anion-templated double helices induced by halogen bonds (XBs) and stabilized by "hydrogen bond enhanced halogen bonds" (HBeXBs). Our findings demonstrate that the number and orientation of hydrogen bond (HB) and XB donors significantly affect the quaternary structure and guest selectivity of two similar oligomers. This research offers new design elements to engineer foldamers and tailor their quaternary structure for specific guest binding.

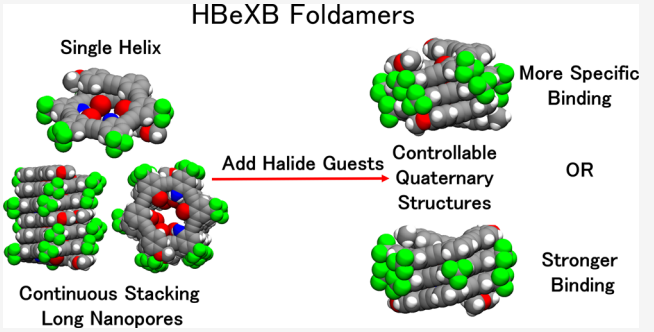

INTRODUCTION

Molecular folding is a fundamental process underpinning an array of critical biological functions, including information storage, signal transduction, catalysis, and selective binding. The significance of molecular folding has driven the creation of synthetic analogues called "foldamers"[1] as materials that emulate and complement the remarkable complexity observed in nature. Synthetic chemists are not constrained by a limited set of building blocks and have developed creative ways to induce secondary structure[2−4] (folding). Many approaches including solvents,[5−10] light,[8,11] pH, rigidity,[12−15] guest templation, anion-π,[16] cation-π,[17] hydrogen bonding (HBing),[18−22] and halogen bonding (XBing) have been developed.[23−27] Furthermore, the well-defined structures and binding pockets of foldamers have enabled unique catalysis,[28] improved biopolymer mimics,[29−33] and specific guest recognition.[18,34]

Anions are environmentally and biologically exciting targets for molecular recognition. However, foldamers designed to bind anions face unique challenges. Anions have diverse topologies, pH dependence, and high free energies of solvation relative to smaller cations. The geometric patterns of anion coordination can largely be explained by the noncovalent interactions between ligands, the topology of the anion (e.g., spherical, linear, planar, or tetrahedral), and the design of the host receptor.[35−37] Many single helix foldamers which bind anions have been developed.[18,19] Still, anion-induced quaternary or higher-order (multistrand) helix assembly in solution remains rare.[18] The association and folding of multiple oligomers, as seen in multimeric proteins, necessitates overcoming significant entropy.[38] Like in proteins, this can be accomplished by enhancing the enthalpy of a binding process, for example, increasing attractive interactions or removing unfavorable repulsions between host and guest, or by increasing overall entropy of a system by desolvation of water from hydrophobic regions.[39] Nevertheless, there are important reasons to design higher-order foldamers. Molecular assemblies with tertiary (involving multiple folding patterns) or quaternary (where multiple strands fold collectively) structures allow for multifunctionality, specific guest binding, and regulation of activity far greater than simpler systems.

Jiang,[40,41] Flood,[42] Li and Zhu,[43,44] Maeda,[45] and Wu[46−50] have pioneered the development of higher-order anion foldamers using hydrogen bonds (HBs). However, there are compelling reasons to explore other noncovalent interactions. The halogen bond (XB) is an alternative interaction that exhibits comparable stabilization energies to HBs while displaying even greater directionality and polarizability.[51,52] We have previously demonstrated the use of XBs to induce quaternary structure, resulting in the first triple-strand Br^- and I^- foldamers.[25,53] Remarkably, these unique structures are stable at temperatures exceeding 68 °C despite the chemical instability of their 4-iodopyridinium monomer units, which

Received: December 30, 2023
Revised: May 2, 2024
Accepted: May 3, 2024
Published: June 6, 2024

https://doi.org/10.1021/jacs.3c14820
J. Am. Chem. Soc. 2024, 146, 16419−16427

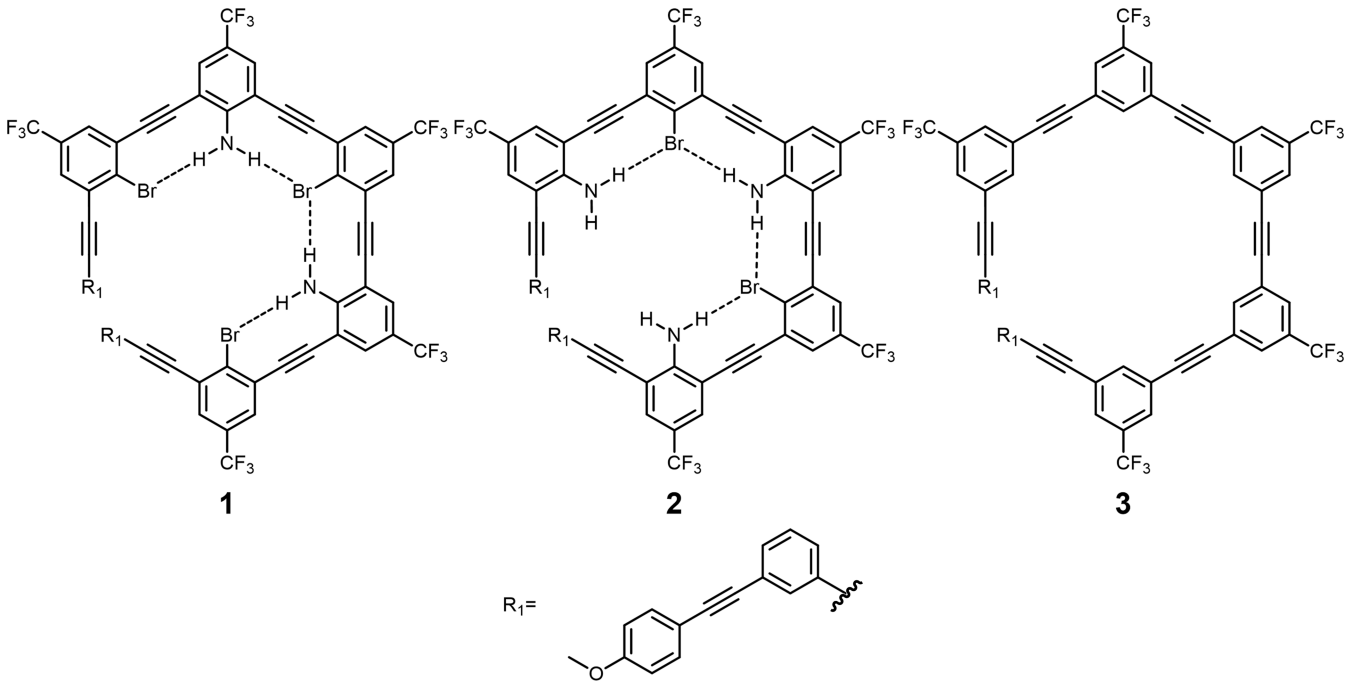

Figure 1. ChemDraw representations of oligomers **1** (left), **2** (middle), and **3** (right). Possible HBeXB interactions have been noted as dashed lines.

readily undergo hydrolysis with residual water in a matter of hours when unfolded.

Subsequently, we also developed the hydrogen bond enhanced halogen bond (HBeXB) which has allowed us to preorganize structure and strengthen XBs by employing complementary intramolecular HBs to the electron-rich belt of XB donors.[54−56] The HBeXB can increase binding by 50-fold[57] and our lab and others have used the HBeXB to improve the function of organocatalysts.[58−60] Ho et al. have also demonstrated that the HBeXB stabilizes protein folding and enhances the function of a T4 lysozyme derivative.[61] Building upon our successes with small molecule HBeXB systems and the formation of complex multistrand XB anion foldamers, we were inspired to employ the HBeXB interaction to create higher-order anion helices. We predicted that an aniline adjacent to a bromobenzene ring in an *m*-phenylethynyl oligomer would induce a helical structure that was internally functionalized with HBeXBs. The HBs to the bromines would promote the folded structure in nonpolar media and enhance the binding strength of the relatively weak bromine XB donors in neutral foldamers. Herein, we created the first HBeXB foldamers and found that the number and orientation of HB and XB donors dictated the quaternary structure of two distinct double helices, which resulted in different anion selectivity and binding strength.

RESULTS AND DISCUSSION

Nonamer **1**, featuring three bromine XB and two NH_2 HB donors, was synthesized using Sonogashira reactions to create an HBeXB foldamer. In this structure, each aniline amino hydrogen could potentially form an HBeXB interaction with a bromine atom on a bromobenzene ring (Figure 1). To investigate the impact of altering the number and position of the HB and XB donors, nonamer **2** was also synthesized, which contains three NH_2 HB donors and two Br XB donors (Figure 1). As a control, molecule **3** was made in a similar fashion to **1** but featured no HB or XB donors and therefore no HBeXB interactions. (Figure 1). Full synthetic details can be found in the Supporting Information (SI).

Small needles of **1** were generated by slow evaporation of **1** in THF-d_8 and studied by single crystal X-ray diffraction. To the best of our knowledge, this is the first X-ray structure of a 9-ring *m*-phenylethynyl foldamer (see SI). **1** crystallized in the $P21/c$ space group with two distinct single strand foldamers in the asymmetric unit. The single helix has a width and height of roughly 24 and 7.2 Å, respectively. The pore of the helix has a diameter of approximately 4.2 Å. **1** coils upon itself with three rings overlapping. One foldamer π-stacks with another, overlapping six rings with the neighboring molecule (Figure 2). The $\pi-\pi$ interactions give rise to foldamer stacks which ultimately produce continuous directional pores that are occupied by disordered THF molecules when viewed along the crystallographic *b* axis. Both molecules in the asymmetric unit exhibit this packing arrangement—the main difference lies in the handedness of the helix formed from the foldamer columns. In the interior, 4 weak HB interactions from aniline protons to bromines (2.91−3.36 Å N−H···Br, 82.7−95.5% $\sum$vdW radii,[62] 166.05−172.76°) further preorganize the single helices. Attempts to crystallize **2** and **3** have so far been unsuccessful.

The foldamers **1**, **2**, and **3** were characterized in solution without guests via ^{1}H, ^{19}F, ^{13}C, HSQC, and HMBC NMR experiments in THF-d_8 (see SI). Folding was characterized by one-dimensional (1D) $^{19}F-^{1}H$ Heteronuclear Overhauser Effect Spectroscopy (HOESY), analyzing the proximity of the foldamer CF_3 groups and phenyl hydrogens. Only HOEs between hydrogens and CF_3 groups of the same phenylic ring were observed for **1**, **2**, and **3**, suggesting that, despite the crystal structure, these strands were not predominantly folded in THF solution. To further investigate folding, deuterium exchange experiments were conducted. The exchange rates of aniline protons were compared between **1** and **2** and their

https://doi.org/10.1021/jacs.3c14820
J. Am. Chem. Soc. 2024, 146, 16419−16427

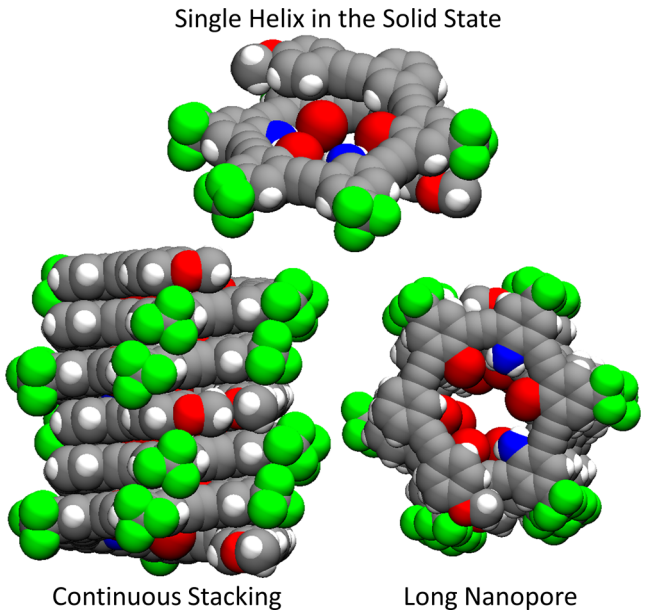

Figure 2. Solid-state structure of single helix **1**. Without anion, this HBeXB foldamer forms single helices (top) and stacks (bottom left) to produce a continuous pore in the solid state (bottom right). Carbons are colored gray, hydrogens white, nitrogens blue, bromines red, and fluorines green. THF is removed for clarity.

respective heptamer counterparts, **28** and **29**, as well as smaller trimer units **13** and **17** which are too small to fold. Notably, the exchange rates of aniline protons were approximately the same for all molecules (see SI page 91). We hypothesize that if the nonamers were folded, the aniline protons would be less accessible to water, slowing down the exchange. However, based on this data, it appears that **1** and **2** maintain some percentage of unfolded conformations in the absence of anions in solution. The solution conformations (folded and unfolded states) of these foldamers are in equilibrium, and the HBeXB could still be influencing the percent foldedness. Furthermore, upon addition of anions, the influence of the HBeXB was later revealed to significantly contribute to the stability of double helix quaternary structures.

To evaluate anion-templated folding of the oligomers, 1D ^{1}H NMR, ^{13}C NMR, and 1D ^{19}F−^{1}H HOESY NMR experiments with anions were performed. Addition of 10 equiv of *N*-tetrabutylammonium bromide (TBABr) in THF-d_8 produced dramatic shifts in all signals. The aromatic protons of **1** were shielded (0.2−0.5 ppm), indicating π-stacking. In contrast, the aniline amine protons were deshielded (0.5 ppm), suggesting increased HBing. Likewise, the carbons attached to the bromine XB donors were also deshielded (approximately 5 ppm for the center ring and 2 ppm for the outer bromobenzene ring), signifying XBing[63] (see SI, Figure S77). The greater XBing-induced deshielding of the center ring XB donor carbon suggested that the Br^- binds near the center ring. The ^{19}F−^{1}H HOESY NMR data revealed heteronuclear Overhauser effects (HOEs) between some anisole ring hydrogens and distant aniline ring fluorine atoms. Additionally, HOE signals were observed between the aniline ring protons and the outer bromobenzene ring trifluoromethyl group (Figure 3). Despite some overlapping signals (see SI, Tables S1−S3) these HOEs could be unambiguously assigned. The observed cross peaks do not correlate with the expected ^{19}F−^{1}H HOESY signals of a single helix (i.e., the crystal structure of **1**) (see SI). Consequently, we hypothesized that an assembly of multiple strands into a higher-order structure (**1_2·Br$^-$**) was formed in the presence of Br^-. DOSY NMR measurements estimated the size of the complex and demonstrated an increase in the hydrodynamic radius (rH) of **1** from 9.6 to 10.4 Å in **1_2·Br$^-$** which aligns with the formation of a new complex.[25,45,46,48]

2 exhibited similar behavior in the presence of TBABr. DOSY NMR identified a change in the molecular radius from 9.4 to 10.4 Å upon the addition of Br^-. All the aromatic ^{1}H NMR resonances of **2** were shielded (0.3−0.7 ppm), while the aniline NH_2 signals were deshielded (0.1 and 0.3 ppm) upon formation of **2_2·Br$^-$**. The ^{13}C resonance attached to the bromine XB donors also became deshielded (4 ppm). However, ^{19}F−^{1}H HOESY NMR revealed a completely

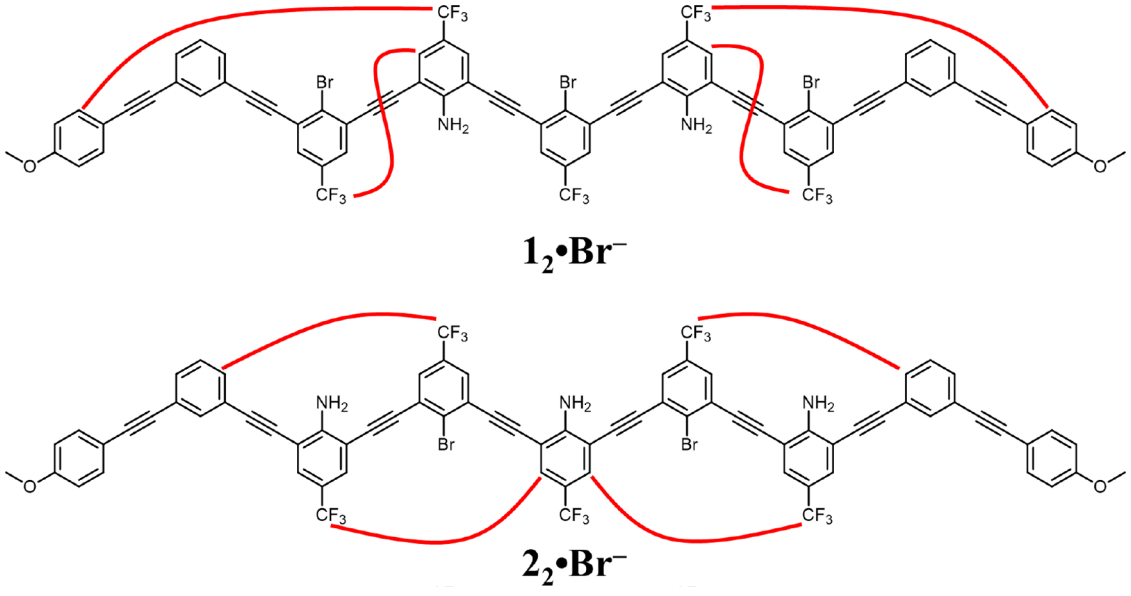

Figure 3. Inter-ring ^{19}F−^{1}H HOEs observed for **1_2·Br$^-$** and **2_2·Br$^-$** in THF-d_8. HOEs are illustrated by red lines.

https://doi.org/10.1021/jacs.3c14820
J. Am. Chem. Soc. 2024, 146, 16419−16427

different set of HOEs than **1**, suggesting a different quaternary structure. One set of HOEs was observed between phenyl ring hydrogens and the trifluoromethyl group of the bromine ring. Another set of HOEs was noted between the center aniline ring hydrogens and the outer aniline ring fluorines (Figure 3). Once again, these HOEs deviated from those expected for a single helix, indicating the presence of a higher-order helix ($\mathbf{2}_2\cdot\mathbf{Br}^-$). These findings confirm that TBABr plays a crucial role in templating the higher-order helices, and that the distinct quaternary structures are influenced by the number and orientation of XB and HB donors.

As anticipated, control **3** did not exhibit any shifting of ^{1}H resonances, inter-ring HOEs, or changes in hydrodynamic radius upon TBABr addition, indicating no binding or folding (see SI). This data indicates that **3** does not bind to Br^- in THF-d_8.

To gain deeper insight, we conducted ^{1}H NMR anion titration experiments. Interestingly, the addition of less than one equivalent of TBABr to both **1** and **2** in THF-d_8 at 25 °C resulted in signal broadening, indicating an intermediate exchange regime that adversely affected the accuracy of the titration.[64] Consequently, the titration experiments were performed at 55 °C under fast exchange conditions. Binding isotherms were evaluated using various models, revealing that both **1** and **2** only conformed to the 2H:1G binding model (see SI)—which we have designated as a d,1-bromide foldamer.[18] **1** showed strong binding to TBABr (K_{11} = 1.4 M^{-1} K_{21} = 5.3 × 10^5 M^{-1}) that was highly positively cooperative, a rarity among anion foldamers[26] (Table 1). **2** displayed an order of magnitude higher binding in a positively cooperative 2:1 stoichiometry to Br^-, reaching the upper limit for NMR titrations (K_{11} = 0.47 M^{-1} K_{21} = 6.3 × 10^6 M^{-1}). These titrations provided further support for the preferred formation of double helices that encapsulate a single Br^- ($\mathbf{1}_2\cdot\mathbf{Br}^-$ and $\mathbf{2}_2\cdot\mathbf{Br}^-$).

Table 1. K_a Values Reported as an Average of Three Titration Experiments of 1 and 2 in THF-d_8 at 55 °C with Halide Anions[a]

guest	K_a for $\mathbf{1}_2\cdot\mathbf{X}^-$ (M^{-1})	K_a for $\mathbf{2}_2\cdot\mathbf{X}^-$ (M^{-1})
TBACl	K_{11} = 2.1 × 10^2	K_{11} = 0.67
	K_{21} = 7.3 × 10^2	K_{21} = 3.3 × 10^6
TBABr	K_{11} = 1.4	K_{11} = 0.47
	K_{21} = 5.3 × 10^5	K_{21} = 6.3 × 10^6
TBAI	K_{11} = 1.0	K_{11} = 1.2
	K_{21} = 3.5 × 10^5	K_{21} = 1.6 × 10^6

[a]Errors[65] estimated at 10% for K_{11} and 25% for K_{21}.

We theorized that cooling down the titration experiments would induce slow exchange. At −40 °C in THF-d_8, **2** exhibited distinct peaks corresponding to the free strand. Upon addition of 0.13 equiv of TBABr, a new set of signals for $\mathbf{2}_2\cdot\mathbf{Br}^-$ emerged in the ^{1}H and ^{19}F NMRs. Notably, these peaks converted into a single host−guest structure ($\mathbf{2}_2\cdot\mathbf{Br}^-$) upon the addition of 0.5 equiv of TBABr, providing compelling evidence for the 2:1 stoichiometry (Figure 4). Similar resonances were seen for **1** forming $\mathbf{1}_2\cdot\mathbf{Br}^-$ under the same conditions. However, the signals never completely resolved to slow exchange (see SI).

Titrations were also conducted with other halides (Table 1). **1** exhibited an element of selectivity, producing binding affinities for I^- and Br^- 3 orders of magnitude greater than Cl^-.

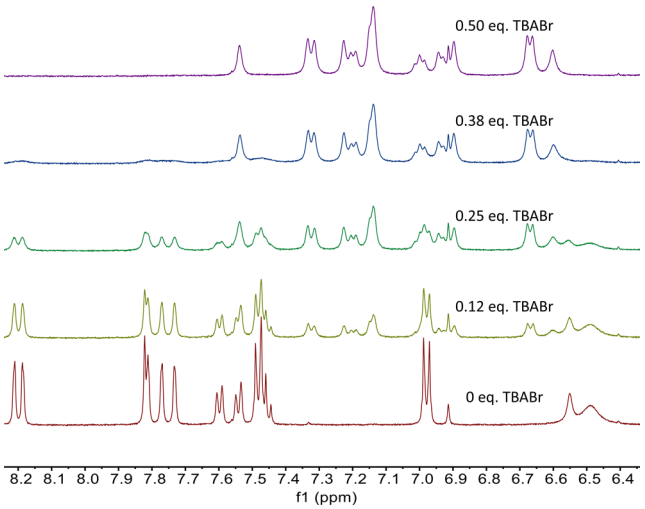

Figure 4. Partial ^{1}H NMR titration experiment for **2** with TBABr at −40 °C in THF-d_8 (0−0.50 equiv TBABr). Slow exchange produced separate signals for **2** and $\mathbf{2}_2\cdot\mathbf{Br}^-$ which resolved to just $\mathbf{2}_2\cdot\mathbf{Br}^-$ at 0.5 equiv (top).

In contrast, **2** displayed stronger binding to each of the halides. We hypothesize that the difference in binding is a consequence of the difference in primary structure, producing a different quaternary structure, for each oligomer which results in a less favorable binding motif for $\mathbf{1}_2\cdot\mathbf{Cl}^-$ relative to $\mathbf{2}_2\cdot\mathbf{Cl}^-$ (see below for further discussion).

Attempts to crystallize the double helices were unsuccessful. Therefore, density functional theory (DFT) models that best represented the HOE contacts from the ^{19}F−^{1}H HOESY NMR experiments were created to visualize $\mathbf{1}_2\cdot\mathbf{Br}^-$ and $\mathbf{2}_2\cdot\mathbf{Br}^-$. To confirm that these were the lowest energy double helices, the strands were also ratcheted into different positions to generate several feasible models that were energetically reasonable but did not correlate with the ^{19}F−^{1}H HOESY data (see SI). Solution data suggested that Br^- interacted strongest with the center-most XB donor in $\mathbf{1}_2\cdot\mathbf{Br}^-$ and bound to the XB donors in $\mathbf{2}_2\cdot\mathbf{Br}^-$, which are located toward the center of each double helix. Therefore, the Br^- was inserted in the center of each model. The structures were optimized using Gaussian-16[66] software and DFT M062X functionals.[67] C, H, O, N, and F atoms were treated with the 6-31g(d) basis set and Br atoms were treated with SDD (ECP28MWB) pseudopotential along with ECP28MWB VTZ basis set. Solvent energy corrections were made using the SMD continuum solvent model[68] with THF as an implicit solvent (see SI). The total energy of formation ($E_{formation}$) for each double helix was calculated using eq 1.

$$E_{formation} = E_{foldamer} - 2 \times E_{single\text{-}strand} - E_{Br^-} \quad (1)$$

$E_{foldamer}$ represents the electronic energy of the fully optimized double helices in the presence of Br^-. $E_{single\text{-}strand}$ is the electronic energy of each DFT-optimized individual free strand. The crystal structure of **1** was used as a starting point for the **1** and **2** $E_{single\text{-}strand}$ calculations. Lastly, E_{Br^-} refers to the electronic energy of the unbound Br^-. Consequently, $E_{formation}$ is the energy difference between $\mathbf{1}_2\cdot\mathbf{Br}^-$ or $\mathbf{2}_2\cdot\mathbf{Br}^-$ and the energies of either **1** or **2** and free $\mathbf{Br}^-$. The models for $\mathbf{1}_2\cdot\mathbf{Br}^-$ and $\mathbf{2}_2\cdot\mathbf{Br}^-$ after DFT calculations were then compared to the HOESY data (Figure 5). Encouragingly, the lowest energy structures obtained from DFT best represented the observed

https://doi.org/10.1021/jacs.3c14820
J. Am. Chem. Soc. 2024, 146, 16419−16427

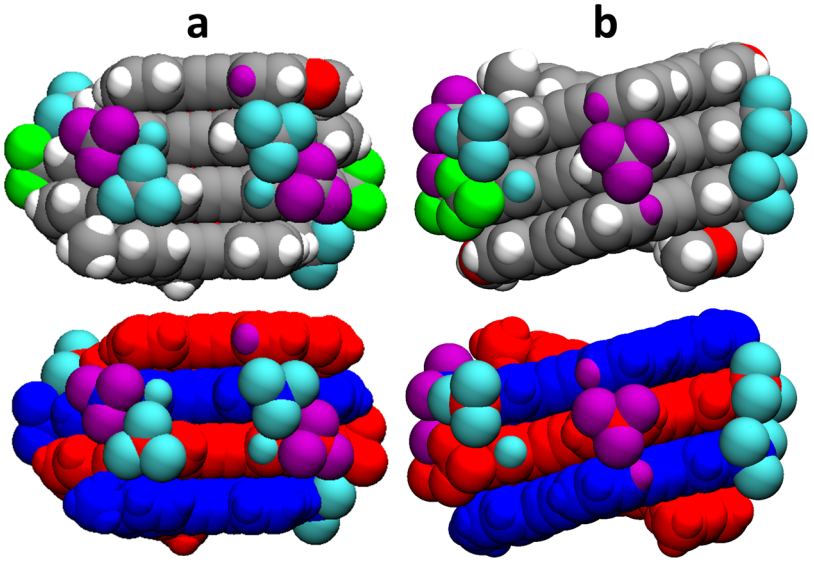

Figure 5. Representations of the lowest energy DFT models of double helices $\mathbf{1}_2\cdot\mathbf{Br}^-$ (a) and $\mathbf{2}_2\cdot\mathbf{Br}^-$ (b), formed in the presence of Br^-. The atoms involved in each of the two inter-ring $^{19}F-^{1}H$ HOESY HOE interactions have been colored teal or purple, respectively. Carbons are colored gray, other hydrogens white, nitrogens blue, bromines red, and other fluorenes green in the top images. In the bottom images, each strand of the double helix is colored red or blue, respectively.

HOESY signals, while higher energy structures did not (see SI, Figures S139 and S140 for all structures).

The computations revealed exciting quaternary structural differences between $\mathbf{1}_2\cdot\mathbf{Br}^-$ and $\mathbf{2}_2\cdot\mathbf{Br}^-$. In $\mathbf{1}_2\cdot\mathbf{Br}^-$ the anisole ring at the end of each strand π-stacks with the outermost bromobenzene ring at one end and the anisole ring at the other, creating a slightly asymmetric structure. In $\mathbf{2}_2\cdot\mathbf{Br}^-$, the anisole ring of one strand π-stacks with the outermost aniline rings of the other strand, which results in a more symmetrical double helix. As expected, the double helical structures of $\mathbf{1}_2\cdot\mathbf{Br}^-$ (approximate average radius of 9.4 Å) and $\mathbf{2}_2\cdot\mathbf{Br}^-$ (approximate average radius of 10.4 Å) are larger than the single helix (7.8 Å, as calculated from the crystal structure of **1**). This increase in size agrees with the trends observed from the DOSY solution experiments (see SI for size calculations). These differences in quaternary structure are small but clearly result in a change in foldamer selectivity and anion guest binding because of the change in their interiors.

Next, the models were analyzed to identify the changes in the binding pocket of each foldamer and rationalize the stronger association of compound **2** with TBABr in solution while justifying the lowest energy structures. Additionally, the energy of double helix formation ($E_{formation}$) was decomposed into three contributions (eq 2) to better understand which forces drive the assembly of $\mathbf{1}_2\cdot\mathbf{Br}^-$ and $\mathbf{2}_2\cdot\mathbf{Br}^-$.

$$E_{formation} = E_{strain} + E_{stacking} + E_{Br^-\text{-binding}} \quad (2)$$

E_{strain} is the bond strain energy required for the strands to bend into the double helix. This is the energy of both strands in the conformation of the optimized double helix structure minus 2 times the energy of the optimized single strand structures. $E_{stacking}$ is the influence of π-stacking in the double helix. This was calculated as the energy of the double helix structures with Br^- removed minus the energy of each strand in the double helix with the other strand and Br^- removed. Finally, $E_{Br^-\text{-binding}}$ accounted for the stabilization due to the interaction of Br^- with each double helix. This was determined as the energy of the double helix structure with Br^- minus the energy of the double helix without Br^- and minus the energy of a free Br^-.

Table 2 presents $E_{formation}$ for $\mathbf{1}_2\cdot\mathbf{Br}^-$ and $\mathbf{2}_2\cdot\mathbf{Br}^-$. The results indicate that both assemble in an exothermic process driven by

Table 2. BSSE-Corrected Formation Energies and Their Components Computed for the Most Stable $\mathbf{1}_2\cdot\mathbf{Br}^-$ and $\mathbf{2}_2\cdot\mathbf{Br}^-$ Complexes Using the M062X Density Functional and the SMD Solvation Model for THF

	$E_{formation}$ kcal mol^{-1}	E_{strain} kcal mol^{-1}	$E_{stacking}$ kcal mol^{-1}	$E_{Br^-\text{-binding}}$ kcal mol^{-1}
$\mathbf{1}_2\cdot\mathbf{Br}^-$	−13.61	58.07	−49.38	−22.30
$\mathbf{2}_2\cdot\mathbf{Br}^-$	−22.67	46.33	−42.78	−26.22

favorable π-stacking ($E_{stacking}$) and XBing interactions to Br^- ($E_{Br^-binding}$). In contrast, the bond strain (E_{strain}) induced by folding into the double helix is unfavorable. The binding energies of $\mathbf{1}_2\cdot\mathbf{Br}^-$ and $\mathbf{2}_2\cdot\mathbf{Br}^-$ show that Br^- binding through XB interactions is a major driving force for double helix assembly. Without Br^- binding, the energy required for folding ($E_{strain} + E_{stacking}$) is unfavorable.

There are several key differences between the quaternary structures of $\mathbf{1}_2\cdot\mathbf{Br}^-$ and $\mathbf{2}_2\cdot\mathbf{Br}^-$. As a result, the binding pockets of each double helix are significantly different, and the binding mode to Br^- reflects this. $\mathbf{1}_2\cdot\mathbf{Br}^-$ exhibits two Br···Br^- XBs (3.25−3.26 Å, 87.3−87.6% ∑vdW radii, 172.3−172.4°) arising from the center XB donors from different oligomers juxtaposed at opposite sides of the Br^-. In contrast, $\mathbf{2}_2\cdot\mathbf{Br}^-$ forms three XBs with Br^- (3.27−3.29 Å 87.9−88.4% ∑vdW radii,[62] 169.5−172.8°), adopting a pseudotrigonal planar arrangement (Figure 6). Additionally, $\mathbf{1}_2\cdot\mathbf{Br}^-$ forms four HB interactions between aniline NH_2 and Br XB donors, while $\mathbf{2}_2\cdot\mathbf{Br}^-$ is stabilized by five intramolecular HBs. As seen in the anion titrations, the extra XB interaction in $\mathbf{2}_2\cdot\mathbf{Br}^-$ serves to increase anion binding while the intramolecular HBs further stabilize the folded state and enhance the additional XB interaction—all leading to a more stable double helix (Table 2). The binding differences are chiefly driven by the variance in

https://doi.org/10.1021/jacs.3c14820
J. Am. Chem. Soc. 2024, 146, 16419−16427

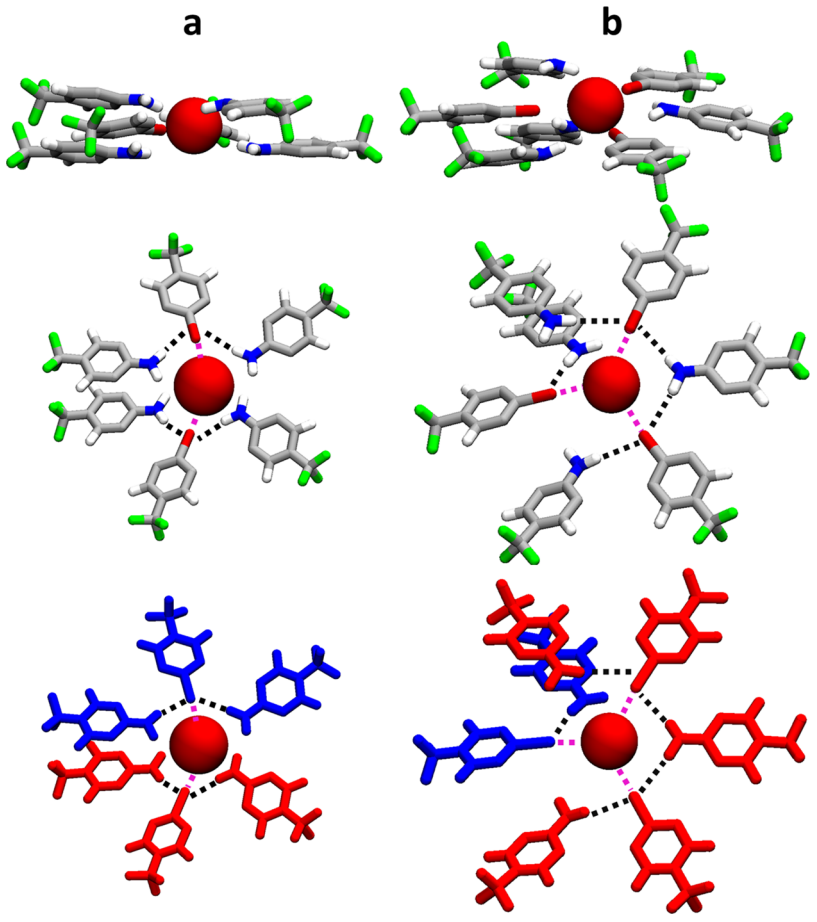

Figure 6. (a) Side (top image) and top view (middle and bottom images) of the XB and HB interactions in $\mathbf{1}_2\cdot\mathbf{Br}^-$. (b) Side (top image) and top view (middle and bottom images) of the XB and HB interactions in $\mathbf{2}_2\cdot\mathbf{Br}^-$. XBs and HBs are represented as magenta and black dashed lines, respectively. Noninteracting residues are not shown for clarity. Carbons are colored gray, hydrogens white, nitrogens blue, bromines red, and fluorines green in the top and middle pictures. In the bottom picture, all atoms from each strand of the double helix are colored red and blue, respectively.

primary structure between the two oligomers. Despite having fewer XB donors per strand, the quaternary structure of $\mathbf{2}_2\cdot\mathbf{Br}^-$ allows for the formation of a binding pocket with three XB donors that favorably interact with Br^-.

We also performed calculations to understand why **2** binds Cl^- strongly in solution, while **1** does not ($K_{21} = 7.3 \times 10^6\ M^{-1}$ and $K_{21} = 3.3 \times 10^2\ M^{-1}$, respectively). Br^- was substituted for Cl^- in the lowest energy $\mathbf{1}_2\cdot\mathbf{Br}^-$ and $\mathbf{2}_2\cdot\mathbf{Br}^-$ models and minimized to create $\mathbf{1}_2\cdot\mathbf{Cl}^-$ and $\mathbf{2}_2\cdot\mathbf{Cl}^-$. As with the solution studies, it was found that $\mathbf{2}_2\cdot\mathbf{Cl}^-$ binds Cl^- stronger than $\mathbf{1}_2\cdot\mathbf{Cl}^-$ (see SI, Table S19). We hypothesize that the arrangement of the two XB donors on *opposite* sides of the helical pore in $\mathbf{1}_2\cdot\mathbf{Cl}^-$ provides a more size selective binding pocket—while Cl^- can still interact with two Br donors, the XBs are weakened due to the smaller van der Waals radius of Cl^-. The XBs in $\mathbf{1}_2\cdot\mathbf{Cl}^-$ (3.21−3.23 Å, 87.2−87.7% ∑vdW radii, C−Br···Cl^- 169.5−171.1°) are longer and less linear than for $\mathbf{2}_2\cdot\mathbf{Cl}^-$. The pseudotrigonal planar arrangement of XB donors in $\mathbf{2}_2\cdot\mathbf{Cl}^-$ allows for two shorter and more linear XB interactions with Cl^- and one slightly longer XB (3.17−3.24 Å, 86.1−88.0% ∑vdW radii, 170.2−172.3°). Another possible explanation is that $\mathbf{1}_2\cdot\mathbf{Cl}^-$ forms a different quaternary structure. Regardless, the influence of the primary structure on the quaternary structure is evident in the difference in binding selectivity between the double helices. Clearly, strategic placement of XB donors in the helical framework has a large influence on the function of the foldamer.

CONCLUSIONS

In this study, we produce the first anion-templated double helices induced by XBs and stabilized by HBeXB interactions. Our findings unveiled that the orientation and number of XB and HB donors on the interior of *m*-phenylethynyl foldamers impact the quaternary structure and function of these systems. In the absence of anions, the foldamers maintained random coil conformations in solution, while **1** crystallized into a single helix with intriguing potential for nanopore applications. Halide binding induced **1** and **2** to form distinct XBing double helices (d,1-halide foldamers).[18] The variation in their primary structures governed the anion-binding capabilities and quaternary structure. **1** selectively bound larger halides, whereas the arrangement of XB and HB interactions in **2** resulted in overall stronger binding to all halide guests in THF-d_8.

From this study it is evident that the strength and quantity of donor functionalities represent only one aspect of controlling higher-order folding and guest binding. Clearly, subtle modification of highly directional noncovalent interactions like XBs can have large consequences in governing the three-dimensional structure of foldamers. In future studies, we

https://doi.org/10.1021/jacs.3c14820
J. Am. Chem. Soc. 2024, 146, 16419−16427

aim to systematically explore how the orientation of XBs and HBs can be tailored to design foldamers with specific structures and properties. This work sets the stage for designing advanced materials and bioinspired machinery, bringing us closer to realizing the full potential of foldamers in practical and real-world applications. Synthetic ion channels, stereoselective catalysts, and transmembrane carriers are among the promising future applications of higher-order foldamers. With continued exploration, these innovative foldamer-based technologies have the potential to address complex molecular design challenges and drive progress in materials science and nanotechnology.

■ ASSOCIATED CONTENT

Supporting Information

The Supporting Information is available free of charge at https://pubs.acs.org/doi/10.1021/jacs.3c14820.

General methods for all studies; synthetic procedures, and characterization for foldamers **1**−**3** and all precursors; methods; and details for deuterium exchange experiments; variable temperature NMR experiments; two-dimensional (2D) NMR experiments, single crystal X-ray diffraction methods and refinement; NMR titration experiments; and computational experiments (PDF)

Accession Codes

CCDC 2284165 contains the supplementary crystallographic data for this paper. These data can be obtained free of charge via www.ccdc.cam.ac.uk/data_request/cif, or by emailing data_request@ccdc.cam.ac.uk, or by contacting The Cambridge Crystallographic Data Centre, 12 Union Road, Cambridge CB2 1EZ, U.K.; fax: +44 1223 336033.

■ AUTHOR INFORMATION

Corresponding Authors

Vyacheslav S. Bryantsev − *Chemical Sciences Division, Oak Ridge National Laboratory, Oak Ridge, Tennessee 37831, United States;* orcid.org/0000-0002-6501-6594; Email: bryantsevv@ornl.gov

Orion B. Berryman − *Department of Chemistry and Biochemistry, University of Montana, Missoula, Montana 59812, United States;* orcid.org/0000-0002-0324-484X; Email: orion.berryman@mso.umt.edu

Authors

Eric A. John − *Department of Chemistry and Biochemistry, University of Montana, Missoula, Montana 59812, United States*

Asia Marie S. Riel − *Department of Chemistry and Biochemistry, University of Montana, Missoula, Montana 59812, United States*

Lianne H. E. Wieske − *Department of Chemistry—BMC, Organic Chemistry, Uppsala University, 752 37 Uppsala, Sweden;* orcid.org/0000-0003-4617-7605

Debmalya Ray − *Chemical Sciences Division, Oak Ridge National Laboratory, Oak Ridge, Tennessee 37831, United States*

Daniel A. Decato − *Department of Chemistry and Biochemistry, University of Montana, Missoula, Montana 59812, United States*

Madeleine Boller − *Department of Chemistry and Biochemistry, University of Montana, Missoula, Montana 59812, United States*

Zoltan Takacs − *Swedish NMR Center, University of Gothenburg, Gothenburg SE-405 30, Sweden*

Máté Erdélyi − *Department of Chemistry—BMC, Organic Chemistry, Uppsala University, 752 37 Uppsala, Sweden;* orcid.org/0000-0003-0359-5970

Complete contact information is available at: https://pubs.acs.org/10.1021/jacs.3c14820

Notes

The authors declare no competing financial interest.

■ ACKNOWLEDGMENTS

The contents of this manuscript have been adapted with permission from a doctoral dissertation.[69] This work was funded by the National Science Foundation (NSF) CHE-2004213, the Center for Biomolecular Structure and Dynamics CoBRE (NIH NIGMS grant P30GM140963). The X-ray crystallographic data were collected using a Bruker D8 Venture, principally supported by NSF MRI CHE-1337908. The work at the Oak Ridge National Laboratory was supported by U.S. Department of Energy, Office of Science, Basic Energy Sciences, Chemical Sciences, Geosciences, and Biosciences Division. This research used resources of the Compute and Data Environment for Science (CADES) at the Oak Ridge National Laboratory and the National Energy Research Scientific Computing Center (NERSC), which are supported by the Office of Science of the U.S. Department of Energy under Contracts No. DE-AC05-00OR22725 and No. DEAC02-05CH11231, respectively.

■ REFERENCES

(1) Gellman, S. H. Foldamers: A Manifesto. *Acc. Chem. Res.* **1998**, *31* (4), 173−180.

(2) Hill, D. J.; Mio, M. J.; Prince, R. B.; Hughes, T. S.; Moore, J. S. A Field Guide to Foldamers. *Chem. Rev.* **2001**, *101* (12), 3893−4011.

(3) Rest, C.; Kandanelli, R.; Fernández, G. Strategies to Create Hierarchical Self-Assembled Structures via Cooperative Non-Covalent Interactions. *Chem. Soc. Rev.* **2015**, *44* (8), 2543−2572.

(4) Le Bailly, B. A. F.; Clayden, J. Dynamic Foldamer Chemistry. *Chem. Commun.* **2016**, *52* (27), 4852−4863.

(5) Suk, J. M.; Jeong, K. S. Indolocarbazole-Based Foldamers Capable of Binding Halides in Water. *J. Am. Chem. Soc.* **2008**, *130* (36), 11868−11869.

(6) Liu, Y.; Parks, F. C.; Sheetz, E. G.; Chen, C. H.; Flood, A. H. Polarity-Tolerant Chloride Binding in Foldamer Capsules by Programmed Solvent-Exclusion. *J. Am. Chem. Soc.* **2021**, *143* (8), 3191−3204.

(7) Hua, Y.; Liu, Y.; Chen, C. H.; Flood, A. H. Hydrophobic Collapse of Foldamer Capsules Drives Picomolar-Level Chloride Binding in Aqueous Acetonitrile Solutions. *J. Am. Chem. Soc.* **2013**, *135* (38), 14401−14412.

(8) Parks, F. C.; Liu, Y.; Debnath, S.; Stutsman, S. R.; Raghavachari, K.; Flood, A. H. Allosteric Control of Photofoldamers for Selecting between Anion Regulation and Double-to-Single Helix Switching. *J. Am. Chem. Soc.* **2018**, *140* (50), 17711−17723.

(9) Kelley, R. F.; Rybtchinski, B.; Stone, M. T.; Moore, J. S.; Wasielewski, M. R. Solution-Phase Structure of an Artificial Foldamer: X-Ray Scattering Study. *J. Am. Chem. Soc.* **2007**, *129* (14), 4114−4115.

(10) De, S.; Chi, B.; Granier, T.; Qi, T.; Maurizot, V.; Huc, I. Designing Cooperatively Folded Abiotic Uni- and Multimolecular Helix Bundles. *Nat. Chem.* **2018**, *10* (10), 51−57.

(11) Hua, Y.; Flood, A. H. Flipping the Switch on Chloride Concentrations with a Light-Active Foldamer. *J. Am. Chem. Soc.* **2010**, *132* (37), 12838−12840.
(12) Hua, Y.; Ramabhadran, R. O.; Karty, J. A.; Raghavachari, K.; Flood, A. H. Two Levels of Conformational Pre-Organization Consolidate Strong CH Hydrogen Bonds in Chloride−Triazolophane Complexes. *Chem. Commun.* **2011**, *47* (21), 5979−5981.
(13) Suk, J.-m.; Kim, D. A.; Jeong, K. S. Helicity Control of an Indolocarbazole Foldamer by Chiral Organic Anions. *Org. Lett.* **2012**, *14* (19), 5018−5021.
(14) Zhao, W.; Wang, Y.; Shang, J.; Che, Y.; Jiang, H. Acid/Base-Mediated Uptake and Release of Halide Anions with a Preorganized Aryl-Triazole Foldamer. *Chem. - Eur. J.* **2015**, *21* (21), 7731−7735.
(15) Shang, J.; Zhao, W.; Li, X.; Wang, Y.; Jiang, H. Aryl-Triazole Foldamers Incorporating a Pyridinium Motif for Halide Anion Binding in Aqueous Media. *Chem. Commun.* **2016**, *52* (24), 4505−4508.
(16) Bornhof, A. B.; Bauzá, A.; Aster, A.; Pupier, M.; Frontera, A.; Vauthey, E.; Sakai, N.; Matile, S. Synergistic Anion−(π) n − π Catalysis on π-Stacked Foldamers. *J. Am. Chem. Soc.* **2018**, *140* (14), 4884−4892.
(17) Craven, T. W.; Cho, M. K.; Traaseth, N. J.; Bonneau, R.; Kirshenbaum, K. A Miniature Protein Stabilized by a Cation−π Interaction Network. *J. Am. Chem. Soc.* **2016**, *138* (5), 1543−1550.
(18) John, E. A.; Massena, C. J.; Berryman, O. B. Helical Anion Foldamers in Solution. *Chem. Rev.* **2020**, *120* (5), 2759−2782.
(19) Juwarker, H.; Jeong, K. S. Anion-Controlled Foldamers. *Chem. Soc. Rev.* **2010**, *39* (10), 3664−3674.
(20) Cao, R.; Rossdeutcher, R. B.; Wu, X.; Gong, B. Oligo(5-Amino-N-Acylanthranilic Acids): Amide Bond Formation without Coupling Reagent and Folding upon Binding Anions. *Org. Lett.* **2020**, *22* (19), 7496−7501.
(21) Huc, I. Aromatic Oligoamide Foldamers. *Eur. J. Org. Chem.* **2004**, *2004* (1), 17−29.
(22) Zhang, D. W.; Zhao, X.; Hou, J. L.; Li, Z. T. Aromatic Amide Foldamers: Structures, Properties, and Functions. *Chem. Rev.* **2012**, *112* (10), 5271−5316.
(23) Zapata, F.; Caballero, A.; Molina, P.; Alkorta, I.; Elguero, J. Open Bis(Triazolium) Structural Motifs as a Benchmark To Study Combined Hydrogen- and Halogen-Bonding Interactions in Oxoanion Recognition Processes. *J. Org. Chem.* **2014**, *79* (15), 6959−6969.
(24) Borissov, A.; Lim, J. Y. C.; Brown, A.; Christensen, K. E.; Thompson, A. L.; Smith, M. D.; Beer, P. D. Neutral Iodotriazole Foldamers as Tetradentate Halogen Bonding Anion Receptors. *Chem. Commun.* **2017**, *53* (16), 2483−2486.
(25) Massena, C. J.; Wageling, N. B.; Decato, D. A.; Martin Rodriguez, E.; Rose, A. M.; Berryman, O. B. A Halogen-Bond-Induced Triple Helicate Encapsulates Iodide. *Angew. Chem., Int. Ed.* **2016**, *55* (40), 12398−12402.
(26) Borissov, A.; Marques, I.; Lim, J. Y. C.; Félix, V.; Smith, M. D.; Beer, P. D. Anion Recognition in Water by Charge-Neutral Halogen and Chalcogen Bonding Foldamer Receptors. *J. Am. Chem. Soc.* **2019**, *141* (9), 4119−4129.
(27) You, L. Y.; Chen, S. G.; Zhao, X.; Liu, Y.; Lan, W. X.; Zhang, Y.; Lu, H. J.; Cao, C. Y.; Li, Z. T. C-H···O Hydrogen Bonding Induced Triazole Foldamers: Efficient Halogen Bonding Receptors for Organohalogens. *Angew. Chem., Int. Ed.* **2012**, *51* (7), 1657−1661.
(28) Girvin, Z. C.; Gellman, S. H. Foldamer Catalysis. *J. Am. Chem. Soc.* **2020**, *142* (41), 17211−17223.
(29) Gopalakrishnan, R.; Frolov, A. I.; Knerr, L.; Drury, W. J.; Valeur, E. Therapeutic Potential of Foldamers: From Chemical Biology Tools To Drug Candidates? *J. Med. Chem.* **2016**, *59* (21), 9599−9621.
(30) Pasco, M.; Dolain, C.; Guichard, G. Foldamers in Medicinal Chemistry. In *Comprehensive Supramolecular Chemistry II*; Elsevier, 2017; pp 89−125.
(31) Baptiste, B.; Godde, F.; Huc, I. How Can Folded Biopolymers and Synthetic Foldamers Recognize Each Other? *ChemBioChem* **2009**, *10* (11), 1765−1767.
(32) Shang, J.; Si, W.; Zhao, W.; Che, Y.; Hou, J. L.; Jiang, H. Preorganized Aryltriazole Foldamers as Effective Transmembrane Transporters for Chloride Anion. *Org. Lett.* **2014**, *16* (15), 4008−4011.
(33) Valkenier, H.; Dias, C. M.; Butts, C. P.; Davis, A. P. A Folding Decalin Tetra-Urea for Transmembrane Anion Transport. *Tetrahedron* **2017**, *73* (33), 4955−4962.
(34) Goto, K.; Moore, J. S. Sequence-Specific Binding of m-Phenylene Ethynylene Foldamers to a Piperazinium Dihydrochloride Salt. *Org. Lett.* **2005**, *7* (9), 1683−1686.
(35) Gale, P. A.; Howe, E. N. W.; Wu, X. Anion Receptor Chemistry. *Chem* **2016**, *1* (3), 351−422.
(36) Hay, B. P. De Novo Structure-Based Design of Anion Receptors. *Chem. Soc. Rev.* **2010**, *39* (10), 3700−3708.
(37) Schmidtchen, F. P. Hosting Anions. The Energetic Perspective. *Chem. Soc. Rev.* **2010**, *39* (10), 3916−3935.
(38) Tamura, A.; Privalov, P. L. The Entropy Cost of Protein Association. *J. Mol. Biol.* **1997**, *273* (5), 1048−1060.
(39) Camilloni, C.; Bonetti, D.; Morrone, A.; Giri, R.; Dobson, C. M.; Brunori, M.; Gianni, S.; Vendruscolo, M. Towards a Structural Biology of the Hydrophobic Effect in Protein Folding. *Sci. Rep.* **2016**, *6* (1), No. 28285.
(40) Yang, L.; Wang, Y.; Che, Y.; Jiang, H. An Aryl-Triazole Foldamer Containing a 1,8-Naphthalimide Fluorescent Motif for Monitoring and Enhancing the Anion-Induced Folding. *Org. Biomol. Chem.* **2017**, *15* (37), 7747−7752.
(41) Wang, Y.; Zhao, W.; Bie, F.; Wu, L.; Li, X.; Jiang, H. Ruthenium(II) Complexes of Aryl Triazole Foldamers as Receptors for Anions. *Chem. - Eur. J.* **2016**, *22* (15), 5233−5242.
(42) Liu, Y.; Parks, F. C.; Zhao, W.; Flood, A. H. Sequence-Controlled Stimuli-Responsive Single-Double Helix Conversion between 1:1 and 2:2 Chloride-Foldamer Complexes. *J. Am. Chem. Soc.* **2018**, *140* (45), 15477−15486.
(43) Li, Y. J.; Xu, L.; Yang, W. L.; Liu, H. B.; Lai, S. W.; Che, C. M.; Li, Y. L. Amidetriazole: A Versatile Building Block for Construction of Oxyanion Anion Receptors. *Chem. - Eur. J.* **2012**, *18* (15), 4782−4790.
(44) Cao, L.; Jiang, R.; Zhu, Y.; Wang, X.; Li, Y.; Li, Y. Synthesis of 1,2,3-Triazole-4-Carboxamide-Containing Foldamers for Sulfate Recognition. *Eur. J. Org. Chem.* **2014**, *2014* (13), 2687−2693.
(45) Maeda, H.; Kitaguchi, K.; Haketa, Y. Anion-Responsive Covalently Linked and Metal-Bridged Oligomers. *Chem. Commun.* **2011**, *47* (33), 9342−9344.
(46) Li, S.; Jia, C.; Wu, B.; Luo, Q.; Huang, X.; Yang, Z.; Li, Q. S.; Yang, X. J. A Triple Anion Helicate Assembled from a Bis(Biurea) Ligand and Phosphate Ions. *Angew. Chem., Int. Ed.* **2011**, *50* (25), 5721−5724.
(47) Wu, B.; Li, S.; Lei, Y.; Hu, H.; Amadeu, N. D. S.; Janiak, C.; Mathieson, J. S.; Long, D. L.; Cronin, L.; Yang, X. J. The Effect of the Spacer of Bis(Biurea) Ligands on the Structure of A2L3-Type (A = anion) Phosphate Complexes. *Chem. - Eur. J.* **2015**, *21* (6), 2588−2593.
(48) Jia, C.; Zuo, W.; Yang, D.; Chen, Y.; Cao, L.; Custelcean, R.; Hostaš, J.; Hobza, P.; Glaser, R.; Wang, Y.; Yang, X. J.; Wu, B. Selective Binding of Choline by a Phosphate-Coordination-Based Triple Helicate Featuring an Aromatic Box. *Nat. Commun.* **2017**, *8* (1), No. 938.
(49) Zuo, W.; Huang, Z.; Zhao, Y.; Xu, W.; Liu, Z.; Yang, X. J.; Jia, C.; Wu, B. Chirality Sensing of Choline Derivatives by a Triple Anion Helicate Cage through Induced Circular Dichroism. *Chem. Commun.* **2018**, *54* (53), 7378−7381.
(50) Bai, X.; Jia, C.; Zhao, Y.; Yang, D.; Wang, S. C.; Li, A.; Chan, Y. T.; Wang, Y.; Yang, X. J.; Wu, B. Peripheral Templation-Modulated Interconversion between an A4L6 Tetrahedral Anion Cage and A2L3 Triple Helicate with Guest Capture/Release. *Angew. Chem., Int. Ed.* **2018**, *57* (7), 1851−1855.

https://doi.org/10.1021/jacs.3c14820
J. Am. Chem. Soc. 2024, 146, 16419−16427

(51) Tepper, R.; Schubert, U. S. Halogen Bonding in Solution: Anion Recognition, Templated Self-Assembly, and Organocatalysis. *Angew. Chem., Int. Ed.* **2018**, *57* (21), 6004−6016.
(52) Cavallo, G.; Metrangolo, P.; Milani, R.; Pilati, T.; Priimagi, A.; Resnati, G.; Terraneo, G. The Halogen Bond. *Chem. Rev.* **2016**, *116* (4), 2478−2601.
(53) Massena, C. J.; Decato, D. A.; Berryman, O. B. A Long-Lived Halogen-Bonding Anion Triple Helicate Accommodates Rapid Guest Exchange. *Angew. Chem., Int. Ed.* **2018**, *57* (49), 16109−16113.
(54) Decato, D. A.; Riel, A. M. S.; May, J. H.; Bryantsev, V. S.; Berryman, O. B. Theoretical, Solid-State, and Solution Quantification of the Hydrogen Bond-Enhanced Halogen Bond. *Angew. Chem., Int. Ed.* **2021**, *60* (7), 3685−3692.
(55) Riel, A. M. S.; Decato, D. A.; Sun, J.; Massena, C. J.; Jessop, M. J.; Berryman, O. B. The Intramolecular Hydrogen Bonded-Halogen Bond: A New Strategy for Preorganization and Enhanced Binding. *Chem. Sci.* **2018**, *9* (26), 5828−5836.
(56) Riel, A. M. S.; Rowe, R. K.; Ho, E. N.; Carlsson, A. C. C.; Rappé, A. K.; Berryman, O. B.; Ho, P. S. Hydrogen Bond Enhanced Halogen Bonds: A Synergistic Interaction in Chemistry and Biochemistry. *Acc. Chem. Res.* **2019**, *52* (10), 2870−2880.
(57) Sun, J.; Decato, D. A.; Bryantsev, V. S.; John, E. A.; Berryman, O. B. The Interplay between Hydrogen and Halogen Bonding: Substituent Effects and Their Role in the Hydrogen Bond Enhanced Halogen Bond. *Chem. Sci.* **2023**, *14* (33), 8924−8935.
(58) Riel, A. M. S.; Decato, D. A.; Sun, J.; Berryman, O. B. Halogen Bonding Organocatalysis Enhanced through Intramolecular Hydrogen Bonds. *Chem. Commun.* **2022**, *58* (9), 1378−1381.
(59) Zhang, Y.; Zhu, H.; Zhang, B.; Yang, H.; Tan, C. H.; Wang, C.; Wen, J.; Zong, L. Hydrogen Bond-Enhanced Halogen Bonding Organocatalyst with C(Sp3)-Br and Sulfoxide Moieties. *ACS Catal.* **2023**, *13*, 7103−7109.
(60) Kaasik, M.; Martõnova, J.; Erkman, K.; Metsala, A.; Järving, I.; Kanger, T. Enantioselective Michael Addition to Vinyl Phosphonatesviahydrogen Bond-Enhanced Halogen Bond Catalysis. *Chem. Sci.* **2021**, *12* (21), 7561−7568.
(61) Carlsson, A. C. C.; Scholfield, M. R.; Rowe, R. K.; Ford, M. C.; Alexander, A. T.; Mehl, R. A.; Ho, P. S. Increasing Enzyme Stability and Activity through Hydrogen Bond-Enhanced Halogen Bonds. *Biochemistry* **2018**, *57* (28), 4135−4147.
(62) Alvarez, S. A Cartography of the van Der Waals Territories. *Dalton Trans.* **2013**, *42* (24), 8617−8636.
(63) Jungbauer, S. H.; Walter, S. M.; Schindler, S.; Rout, L.; Kniep, F.; Huber, S. M. Activation of a Carbonyl Compound by Halogen Bonding. *Chem. Commun.* **2014**, *50* (47), 6281−6284.
(64) Thordarson, P. Determining Association Constants from Titration Experiments in Supramolecular Chemistry. *Chem. Soc. Rev.* **2011**, *40* (3), 1305−1323.
(65) Hibbert, D. B.; Thordarson, P. The Death of the Job Plot, Transparency, Open Science and Online Tools, Uncertainty Estimation Methods and Other Developments in Supramolecular Chemistry Data Analysis. *Chem. Commun.* **2016**, *52* (87), 12792−12805, DOI: 10.1039/c6cc03888c.
(66) Frisch, M. J.; Trucks, G. W.; Schlegel, H. B.; Scuseria, G. E.; Robb, M. A.; Cheeseman, J. R.; Scalmani, G.; Barone, V.; Petersson, G. A.; Nakatsuji, H.; Li, X.; Caricato, M.; Marenich, A. V.; Bloino, J.; Janesko, B. G.; Gomperts, R.; Mennucci, B.; Hratchian, H. P.; Ortiz, J. V.; Izmaylov, A. F.; Sonnenberg, J. L.; Williams-Young, D.; Ding, F.; Lipparini, F.; Egidi, F.; Goings, J.; Peng, B.; Petrone, A.; Henderson, T.; Ranasinghe, D.; Zakrzewski, V. G.; Gao, J.; Rega, N.; Zheng, G.; Liang, W.; Hada, M.; Ehara, M.; Toyota, K.; Fukuda, R.; Hasegawa, J.; Ishida, M.; Nakajima, T.; Honda, Y.; Kitao, O.; Nakai, H.; Vreven, T.; Throssell, K.; Montgomery, J. A., Jr.; Peralta, J. E.; Ogliaro, F.; Bearpark, M. J.; Heyd, J. J.; Brothers, E. N.; Kudin, K. N.; Staroverov, V. N.; Keith, T. A.; Kobayashi, R.; Normand, J.; Raghavachari, K.; Rendell, A. P.; Burant, J. C.; Iyengar, S. S.; Tomasi, J.; Cossi, M.; Millam, J. M.; Klene, M.; Adamo, C.; Cammi, R.; Ochterski, J. W.; Martin, R. L.; Morokuma, K.; Farkas, O.; Foresman, J. B.; Fox, D. J. *Gaussian 16, Revision 01C*; Gaussian, Inc.: Wallingford CT, 2016.
(67) Zhao, Y.; Truhlar, D. G. The M06 Suite of Density Functionals for Main Group Thermochemistry, Thermochemical Kinetics, Noncovalent Interactions, Excited States, and Transition Elements: Two New Functionals and Systematic Testing of Four M06-Class Functionals and 12 Other Function. *Theor. Chem. Acc.* **2008**, *120* (1−3), 215−241.
(68) Marenich, A. V.; Cramer, C. J.; Truhlar, D. G. Universal Solvation Model Based on Solute Electron Density and on a Continuum Model of the Solvent Defined by the Bulk Dielectric Constant and Atomic Surface Tensions. *J. Phys. Chem. B* **2009**, *113* (18), 6378−6396.
(69) John, E. A. Leveraging Hydrogen Bond enhanced Halogen Bonding for Higher-Order Anion Helix Formation in Foldamers. Ph.D. Thesis, University of Montana: Missoula, MT, 2024.